Earth and Planetary Science Letters 269 (2008) 518–522

Contents lists available at ScienceDirect

Earth and Planetary Science Letters

journal homepage: www.elsevier.com/locate/epsl

Extensive perched aquifer and structural implications revealed by 3D resistivity mapping in a Galapagos volcano ☆

Noémi d'Ozouville [a], Esben Auken [b], Kurt Sorensen [b], Sophie Violette [a,*], Ghislain de Marsily [a], Benoit Deffontaines [c], Godfrey Merlen [d]

[a] Université Pierre et Marie Curie, UMR.7619-Sisyphe, 4, Place Jussieu, 75252 Paris, Cedex 05, France
[b] HydroGeophysics Group, Department of Earth Sciences, University of Aarhus, Høegh-Gulbergs gade 2, DK-8000 Århus, Denmark
[c] Université de Marne-la-Vallée, Laboratoire Géomatériaux et Géologie de l'Ingénieur, 5 Bd. Descartes, Champs-sur-Marne, F-77454 Marne-la-Vallée, Cedex 2, France
[d] Galapagos National Park Service, Puerto Ayora, Santa Cruz Island, Galapagos, Ecuador

ARTICLE INFO

Article history:
Received 16 November 2007
Received in revised form 29 February 2008
Accepted 3 March 2008
Available online 15 March 2008

Editor: C.P. Jaupart

Keywords:
geophysics
groundwater
landslide
transient electromagnetic

ABSTRACT

Due to the complexity of geological formations and limited subsurface data in volcanic islands, hydrogeological conceptual models can differ from one island to another and for the same island. The Galapagos Islands, like most inhabited volcanic islands, face important water resource problems which might have a major impact on their unique and pristine ecosystems, Endanger World Heritage list (June 2007). The scarcity of geological and hydrological data combined with the difficulty of access for field measurements lead to a poor understanding of the island hydrogeology and unconvincing interpretation of traditional geophysical data. Here we present three dimensional (3-D) resistivity maps for the supposedly "waterless" Santa Cruz Island, obtained by using the SkyTEM device, a helicopter-borne transient electromagnetic method. The latter is non-invasive and measurements over inaccessible terrain were of vital importance. We show that even in high-relief terrain with extreme subsurface resistivity contrasts [1-6 000 ohm-m], the method is sensitive to low-resistivity layers of hydrogeological interest [50-200 ohm-m] to a depth of approximately 300 m. The unique spatial resolution and 3-D view of the subsurface resistivity structures allow identification of two zones of hydrogeological importance: a previously unknown extensive perched aquifer (50 km^2) on the southern mountain side and the geometry of the salt-water wedge in the basal aquifer located with an accuracy of a few meters. This finding supports the existence of hidden perched aquifers on basaltic islands, until now only inferred from hydrogeological studies. It is seen to be affected by faulting. Beyond the vital implications for water resource and ecosystem management in the unique yet severely threatened Galapagos Islands, some conceptual flow models of volcanic islands have to be reconsidered. The presence of such structures in a volcanic edifice recognized as low strength layer may help to explain the origin of potentially catastrophic landslides.

1. Introduction

The rapid growth of the human population on the "waterless" volcanic island of Santa Cruz in the Galapagos (Fig. 1a) demands an urgent investigation into its hydrological system to avoid ecosystem alterations and provide viable solutions to the increasing water demand. This island covers an area of 986 km^2, has 13 000 inhabitants (6000 people/km^2 in the main urbanization) and 120 000 visitors per year, but shows no signs of groundwater resources other than a small seep from a scoria cone in the highlands (0.01-0.1 L/s) and a tide-influenced brackish basal aquifer (electrical conductivity of water: 1-7 mS/cm; water level 5 km inland: 0.5 m above sea level (m a.s.l.)). From June to December, the cool south-east trade winds create a persistent wet inversion layer from 250 m a.s.l. to the summit of the island at 855 m a.s.l., yielding greater hydrogeological potential on the windward mountainside. From January to June, the maximum orographic rainfall from variable moisture-laden winds occurs in the same area.

Our study was designed to obtain a high resolution three-dimensional (3-D) view of the internal resistivity structure of Santa Cruz Island that would reveal unknown details of the subsurface and the hydrogeology, supplying data where none was previously available (Colinvaux, 1968). Non-invasive surveying of National Park land (70% of Santa Cruz land surface) and the ability to fly over inaccessible terrain were of vital importance. Interpretation of ground based geophysical measurements is of limited values due to the scarcity of data, whereas the 3-D resistivity structures obtained here by the helicopter-borne transient electromagnetic

☆ All authors contributed equally to the work.
* Corresponding author. Tel.: +33 1 44 27 51 30; fax: +33 1 44 27 51 25.
E-mail addresses: noemi_doz@yahoo.com (N. d'Ozouville), esben.auken@geo.au.dk (E. Auken), kurt.sorensen@geo.au.dk (K. Sorensen), sophie.violette@upmc.fr (S. Violette), GDemarsily@aol.com (G. de Marsily), benoit.deffontaines@univ-mlv.fr (B. Deffontaines), merlenway@gmail.com (G. Merlen).

0012-821X/$ – see front matter © 2008 Elsevier B.V. All rights reserved.
doi:10.1016/j.epsl.2008.03.011

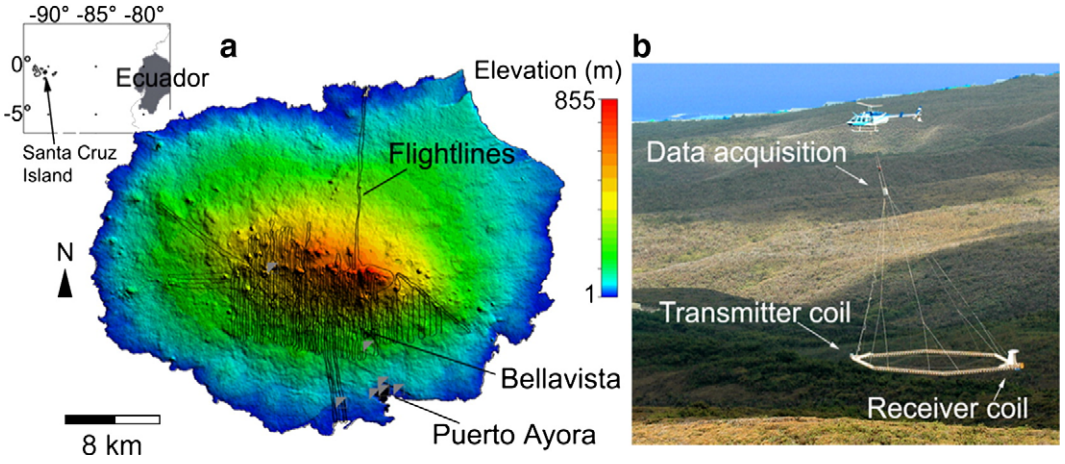

Fig. 1. Overview map showing the Santa Cruz Island, the SkyTEM flight lines and SkyTEM system in operation. a) Santa Cruz is a central island in the Galapagos Archipelago (inset). Shown are the limited permanent water resources of the island (◩): a unique low-outflow, highland spring (450 m a.s.l.), a single deep brackish water well (elevation: 160 m a.s.l.), and coastal open fractures called "grietas" with brackish contaminated water (elevation: 5-15 m a.s.l.). Data acquisition flight lines carried out during the SkyTEM survey are shown in black over topography (DEM from (d'Ozouville et al., in press)). b) SkyTEM instrumentation hangs in a rig 30 m below the helicopter which flies 60-75 m above the ground surface at a speed of 45 km/hour on average.

method, SkyTEM (Sørensen and Auken, 2004) (Fig. 1b), give sufficient insight to understand the internal structure of the volcano. Over 900 km of profile transient data (covering an area of approximately 190 km^2) were gathered in 8 days (Fig. 1a).

2. Methods

SkyTEM (Sørensen and Auken, 2004) is a transient electromagnetic system where weak subsurface currents are induced by a very strong current flowing in the transmitter coil. The subsurface currents diffuse into the ground with a magnitude and decay which are related to the conductivity of the geological layers (Fitterman and Labson, 2005). The data which is measured in the receiver coil (Fig. 1b) is the time derivative of the magnetic field from the decaying subsurface currents. Average helicopter flying speed was 45 km/h during the Santa Cruz survey and the flight altitude of the rig was 35-45 m. In general lines were oriented South–North and the average spacing were 200 m. A few lines were flown cross island to obtain a full picture of the salt-fresh water interface. Navigation data (flight altitude, tilt of the frame, GPS position) are processed and the data itself are filtered by trapezoid-shaped filters (Auken et al., 2007) in order to suppress natural background noise. The filters were designed to enhance near-surface resistivity variations by avoiding any smoothing of the early time data. At later times data were more severe filtered to obtain as much depth penetration as possible. After filtering, data are gathered into soundings with a spatial distance of about 25 m. The inversion model is described by a number of layers, each with a thickness and a resistivity (Auken and Christiansen, 2004). The soundings are inverted using the

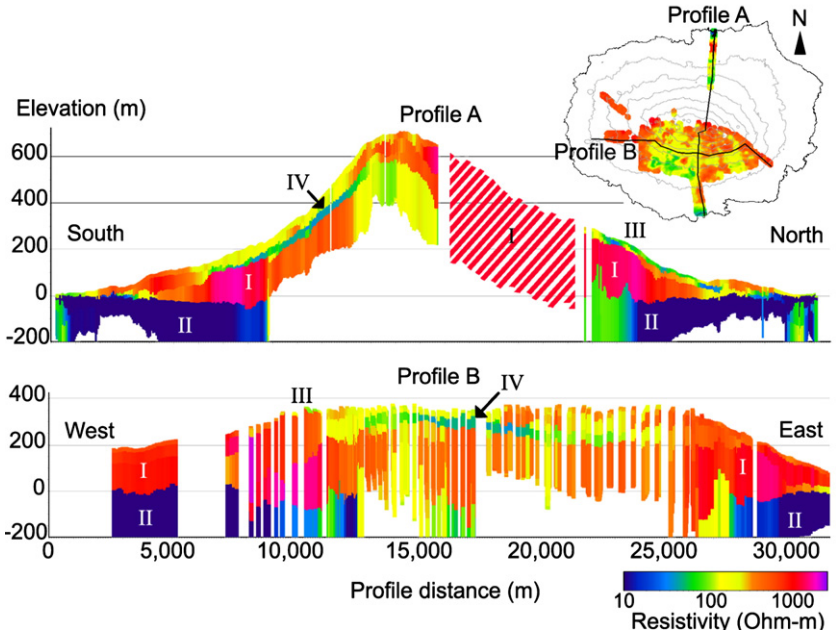

Fig. 2. Two cross-sections reveal the internal structure of Santa Cruz Island and four units of hydrogeological interest. The positions of the south-north and west-east profiles across the island are shown on the inset over a background of near-surface average resistivity showing extent of mapped area. The profiles show the density of data generated and the penetration depth of between 200 and 300 m. The four units of hydrogeological interest are: (I) High-resistivity unsaturated basalts; (II) Seawater intrusion wedge underlying the brackish basal aquifer; (III) Near-surface, low-resistivity units consisting of colluvial deposits; (IV) Internal, low-resistivity unit of saturated basalts overlying an impermeable stratum.

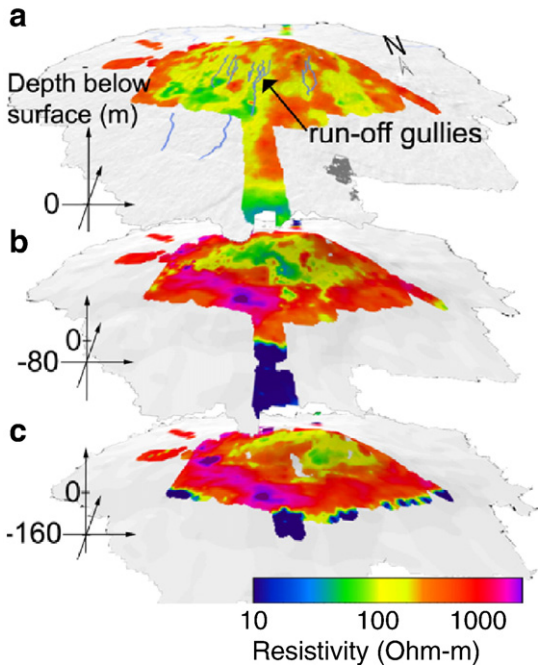

Fig. 3. Three-dimensional visualization of the internal resistivity structure of Santa Cruz Island. a) 0-20 m near-surface average resistivity map draped over the surface topography shows the coincidence of low-resistivity zones with run-off gullies. b) 80-100 m below surface average resistivity map shows the extent of the internal low-resistivity unit on the windward side of the volcano, surrounded by unsaturated basalts; the inland extent of the seawater wedge is clearly visible as the dark blue area. c) 160-180 m below surface average resistivity map shows the disappearance of the low-resistivity unit to the east and the further inland extent of the seawater wedge.

spatially constrained inversion (SCI) technique (Viezzoli et al., in press) which results in a quasi 3D model of the subsurface resistivity structures. Because the technique uses local 1D derivatives it does not track very sharp lateral resistivity changes and these will to some degree be smeared out in the final maps. Individual depth-resistivity soundings along flight lines are represented in 2-D cross-sections (Fig. 2) and spatial interpolation using kriging are carried out to generate 3-D views in terms of average resistivity at depths below the topographic surface (Fig. 3). This is in agreement with the conic layered construction of the volcanic edifice.

3. Results

Inversion results plotted along two cross-sections of the island are shown in Fig. 2. A range of resistivity values varying from 1 to 6000 Ω m is used to define four hydrogeological units reaching a maximum depth of 300 m (Fig. 2): (I) end-member unit with values >800 Ω m representing unsaturated fractured basalts (Descloitres et al., 1997; Albouy et al., 2001) and (Lénat et al., 2000), (II) end-member unit with resistivity values <10 Ω m corresponding to fractured basalts invaded by seawater (Descloitres et al., 1997; Albouy et al., 2001) and (Lienert, 1991), (III) near-surface and (IV) buried units with resistivity values ranging from 50 to 200 Ω m, that are potentially weathered zones or fractured basalts saturated with freshwater (Descloitres et al., 1997; Lienert, 1991) and (Krivochieva and Chouteau, 2003). Spatial interpolation of the resistivity profiles permits 3-D visualization of the units (Fig. 3), the characterization of their geometry and interpretation of their hydrogeological significance.

Unit I (>800 Ω m shown in red) dominates the northern mountainside (Fig. 2) and is also present on the southern one, comprising more than 50% of the mapped area (Fig. 3). Consistent with resistivity ranges found in the literature (Descloitres et al., 1997; Albouy et al., 2001) and (Lénat et al., 2000), these high resistivity values exclude any possibility of water saturation and validate the characterization of the unit as thick unweathered, unsaturated flows of alkali basalts that make up the bulk of the Santa Cruz volcano. Indeed, the construction of the subaerial volcanic shield, dated between 1.12 (±0.07) to 0.024 (±0.011) myr. (White et al., 1993), reveals no large gaps in volcanic activity or major eruptions of differentiated material. Though initially impermeable, these basalts develop a high secondary permeability from cooling joints and tectonic fracturing.

Unit II (<10 Ω m shown in dark blue) is located near sea level on all sides of the volcano (Fig. 2). It represents the salt-water wedge beneath the island, formed by lateral seawater intrusion into the fractured basalts below the basal aquifer. The unit slopes inland from the coast on the eastern and southern sides and is no longer detected when its distance from the ground surface exceeds the maximum penetration depth of the SkyTEM system (300 m) approximately 9 km inland. This shows how the highly fractured nature of the basalts allows continuous seawater intrusion and gives an unprecedented view of the geometry of the salt-water wedge beneath an island (Descloitres et al., 1997). The inverse hydraulic gradient of 0.004 at the top of the salt-water wedge on the southern side of the volcano (Fig. 2) is consistent with the known presence of a thin fresh-water lens on top of the salt-water. It is in close agreement with the Ghyben-Herzberg formula (Vacher, 1988), stating that the salt-water/fresh-water interface is located at a depth below sea level of forty times the elevation of the head above sea level, and the 0.0001 hydraulic gradient of this fresh-water lens as observed at the only one bore well located 5 km inland (Fig. 1). This result allows an extrapolation of this water lens to the whole island, whereas previously water levels were only known where they had been measured, i.e. in the bore well and in coastal fractures connected to the sea (Fig. 1a).

Outcrop Unit III (50-200 Ω m shown in blue-green to yellow) consists of near-surface, low-resistivity zones that outcrop on both the north and the south sides of the volcano (Fig. 2). Although the unit has the same resistivity range as Unit IV, the interpretation differs based on existing geological and geomorphological data. To the south these zones coincide with non-perennial hydrological runoff gullies (Fig. 3a) and identified colluvial deposits (INGALA, ORSTOM, PRONAREG, 1987), both indicating the presence of erodable surfaces such as weathered horizons. Below ~150 m a.s.l. the gullies disappear. This may be due to sediment load becoming superior to water discharge flux and/or preferential vertical infiltration through fractured basalts at the lower limit of the weathered zone. The presence of a thin and restricted low resistivity zone on the northern mountainside further support the colluvial origin of this unit as runoff occurs there only during exceptional El Niño events (rain from the west) and weathering is extremely low. The resistivity range of this unit reflects the heterogeneous nature of the deposits as resistivity is a function of porosity, water saturation, solute content and presence of clay (Palacky, 1988).

Buried Unit IV (50-200 Ω m shown in blue-green to yellow) is of great hydrogeological interest. The resistivity range of the unit is consistent with that observed on other islands for freshwater-saturated basalts (Descloitres et al., 1997; Lienert, 1991) and (Krivochieva and Chouteau, 2003). It forms a distinctive internal low-resistivity zone present exclusively in the upper section of the southern side of the volcano (Fig. 2, Fig. 3b). The single unit, over 50 km^2 in extent, is wedge-shaped along an N-S axis: 80 m thick upslope and <10 m down slope and gently dips from west to east (Fig. 2).

Abrupt voltage changes observed in the raw data processing correspond with surface fractures and east–west trending faults with up to 30 m of vertical displacement. In the inversion models, these faults are seen to affect and offset vertically the structure of this low-resistivity layer (Fig. 4a). While some faults extend at depth from the surface, others that are not visible on the surface will have been covered by younger lava flows, colluvial deposits, weathering and vegetation. The 3-D view (Fig. 4) of the unit shows that it is quasi-parallel to the topography and coincides with the area of maximum

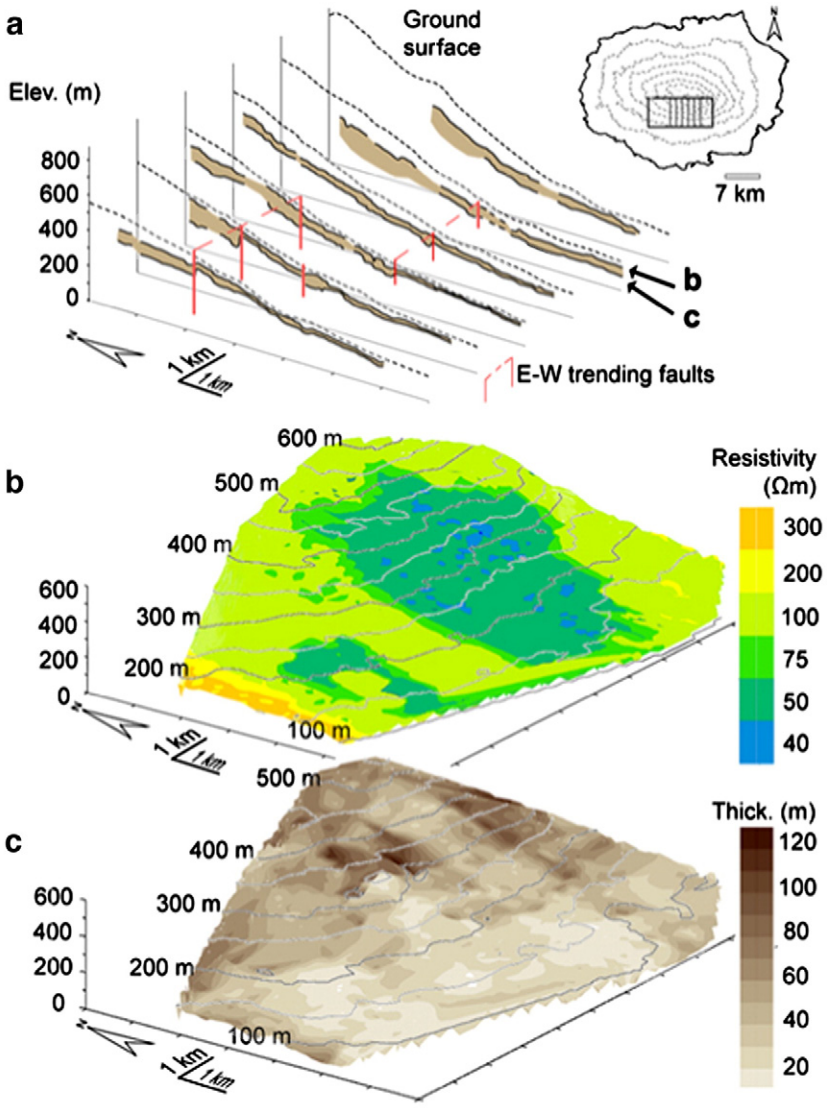

Fig. 4. Three-dimensional visualization of the resistivity and geometry of the zone of hydrogeological interest: interpreted as the hidden perched aquifer. a) Perspective view of the 3-D geometry of the internal low-resistivity zone buried at mid-altitude on the windward side of the island. The inset shows the area of focus and selected profiles. This unit, quasi-parallel to the topography with no visible outcrop, is believed to be coeval with the formation of the volcanic massif. Its extent, thickness and nature reveal high potential for a groundwater reservoir fed by diffuse infiltration of meteoric water. The location of E-W trending faults is marked by the sharp vertical offsets in the low-resistivity layer. b) Resistivity range overlain on the roof surface of the perched aquifer layer shows the area with greatest hydrogeological potential. c) Thickness of the perched aquifer layer overlain on the relief of its wall shows this layer dipping east and thinning down-slope and to the west.

rainfall and air moisture reflected by the vegetation distribution (White et al., 1993). This suggests that the origin of the unit is coeval with the building phases of the volcano and related to the hydrous potential. This unit does not outcrop on the generated geophysical maps and profiles and is not observed in the field. The lack of surface springs therefore does not exclude the presence of an aquifer. Furthermore, the presence of the identified large-scale faults will facilitate internal drainage which would help explain the absence of surface seepage. High altitude groundwater exists in a similar geologic context on nearby San Cristobal Island.

4. Discussion

Geological and climatological evidence is consistent with the presence of this hidden, perched aquifer. The resistivity range of Unit IV is realistically explained as being composed of the same basalts as those of Unit I, but underlain by an impermeable layer that allows their saturation. A thin impermeable layer (<5 m) is geophysically unresolved and results in an effective single layer of average resistivity with the saturated basalts (Jorgensen et al., 2003). Baked soils, known as "red beds", are common impermeable layers within volcanic massifs (Coudray et al., 1990) and (Custodio, 2005). They are observed on the sea-cliffs of north-eastern Santa Cruz and southern San Cristobal. Two probable origins of the impermeable layer exist. (i) The first is a "single 2-3 m irregular thick blanket of comminuted ash" deposited in the south during an explosive phase of volcanism towards the end of the "shield building phase" (Bow, 1979). This pyroclastic material, readily weathered to clay with low intrinsic permeability, was baked by lava flows generated in the re-activation of the summit cones and fissure system during the "shield modifying stage" (Bow, 1979). (ii) The second is the baking of a succession of accumulated allochthonous colluvial deposits that were transformed by heat from overriding lava flows during the volcanic building process. The result is an extensive patchwork of permeable–impermeable layers in which water accumulates. Other lithological hypotheses, including thick pyroclastic deposits, unsaturated basalts with lower resistivity and thick saturated impermeable clays, are not consistent with the known volcanic history of Santa Cruz Island.

Available historical climatological data (Huttel, 1995) give an average rainfall on the southern slope from 500 mm/yr on the coast to 1800 mm/yr at 600 m. During El Niño years the rainfall can more than triple (Snell and Rea, 1999) enhancing the diffuse infiltration to recharge the unconfined perched aquifer. Measured soil hydraulic conductivities are favorable for infiltration process to occur (10^{-6} to 10^{-4} m/s, increasing with lower altitude) (Adelinet et al., 2008). We consider that the top of the low-resistivity zone (Fig. 4b) corresponds to the top of the water table within the perched aquifer, which results in a hydraulic gradient of 0.06. The saturated zone ends abruptly 7.7 km inland 20 m below the ground surface. The water from the perched aquifer is assumed to recharge the basal aquifer through faults, which allow rapid flow. As a saturated and potentially weathered layer, the base of the perched aquifer (Fig. 4c) represents an excellent basal detachment surface for the occurrence of landslides, such as those affecting other volcanic islands of the archipelago (Geist et al., 2002) and (Naumann and Geist, 2000). Such landslides may be triggered by the reactivation of seismic and/or volcanic activity. Santa Cruz should still be considered as active as it has erupted in the Holocene (White et al., 1993).

5. Conclusions

These results show that Santa Cruz Island is not as “waterless” as previously thought due to the absence of surface indicators of the hidden perched aquifer. The local implications of this finding are the changed dynamics of the hydrological regime. Although perched aquifers have been inferred on other volcanic islands based on alignment of springs (Stieljes, 1988), geological outcrops (Custodio, 2005), geochemistry (Nascimento Prada et al., 2006) and (Cruz and França, 2006) or modeling (Violette et al., 1995), they have never been thoroughly mapped nor visualized in 3-D. Some conceptual flow models (Peterson, 1972; Custodio et al., 1988; Hildenbrand et al., 2005) and (Join et al., 2005) will have to be reconsidered to allow for such structures to exist and for their potentially great extent whereas until now they were considered only to be localized small scale features of limited interest. The extent and continuity of the newly discovered hidden perched aquifer gives unprecedented weight to their role in relation with large landslide occurrences on old volcanic island edifices (Hürlimann et al., 1999) and (Malheiro, 2006) and to inducing phreatomagmatic eruptions on active volcanoes. Our results bring a new slant to Galapagos natural history, highlighting that the adaptation and evolution of species have also occurred on the basis of a particular hydrogeological setting, thus providing a link between the physical earth and the organisms that live there.

Acknowledgments

We thank the Galapagos National Park Service, the Charles Darwin Foundation, the Municipality of Santa Cruz and the Galapagos National Institute for local collaboration and logistics; and Fondation de France, Fondation Véolia Environnement, Fondation Schlumberger-SEED, Chancellerie des Universités de Paris, UGAFIP-BID and Municipality of Santa Cruz for financial support. We thank K. Beven, C. Jaupart, L. Pellerin and A. Christiansen for comments.

References

Adelinet, M., Fortin, J., d'Ozouville, N., Violette, S., 2008. The relationship between hydrodynamic properties and weathering of soils derived from volcanic rocks - Galapagos Islands (Ecuador). Environ. Geol. doi:10.1007/s00254-007-1138-3.

Albouy, Y., Andrieux, P., Rakotondrasoa, G., Ritz, M., Descloitres, M., Join, J.-L., Rsolomanano, E., 2001. Mapping coastal aquifers by joint inversion of DC and TEM sounding, three case histories. Groundwater 39, 87–97.

Auken, E., Christiansen, A.V., 2004. Layered and laterally constrained 2D inversion of resistivity data. Geophysics 69, 752–761.

Auken, E., Westergaard, J., Christiansen, A.V., Sørensen, K.I., 2007. Processing and inversion of SkyTEM data for high resolution hydrogeophysical surveys. Proceedings of the Australian Society of Exploration Geophysics meeting in Perth. 4p.

Bow, C.S., 1979. Geology and Petrogenesis of Lavas from Floreana and Santa Cruz Islands, Galapágos Archipelago. Ph.D. thesis Univ. Oreg.

Colinvaux, P., 1968. Reconnaissance and Chemistry of the Lakes and Bogs of the Galapagos Islands. Nature 219, 590–594.

Coudray, J., Mairine, P., Nicolini, E., Clerc, J.M., 1990. Approche hydrogéologique. In: Lénat, J.F. (Ed.), Le volcanisme de l'île de la Réunion, Centre de Recherches Volcanologiques, Clermont-Ferrand.

Cruz, V.J., França, Z., 2006. Hydrogeochemistry of thermal and mineral water springs of the Azores archipelago (Portugal). J. Volcanol. Geotherm. Res. 151, 382–398.

Custodio, E., 2005. Hydrogeology of volcanic rocks, in: Groundwater studies. An international guide for hydrogeological investigations, UNESCO (Eds), Paris.

Custodio, E., Lopez Garcia, L., Amigo, E., 1988. Simulation par modèle mathématique de l'Ile volcanique de Ténériffe, (Canaries, Espagne). Hydrogéol. 2, 153–167.

Descloitres, M., Ritz, M., Robineau, B., Courteaud, M., 1997. Electrical structure beneath the eastern collapsed flank of Piton de la Fournaise volcano, Reunion Island: implications for the quest of groundwater. Water Resour. Res. 33, 13–19.

d'Ozouville, N., Deffontaines, B., Benveniste, J., Wegmuller, U., Violette, S., de Marsily, G., in press. DEM generation using ASAR (ENVISAT) for addressing the lack of freshwater ecosystems management, Santa Cruz Island, Galapagos. Remote Sensing of Environment on Monitoring Freshwater Ecosystems, special issue.

Fitterman, D.V., Labson, V.F., 2005. Electromagnetic induction methods for environmental problems. In: Butler, D.K. (Ed.), Near-surface Geophysics Part I. Society of Exploration Geophysicists, Tulsa.

Geist, D.J., White, W.M., Albarède, F., Harpp, K.S., Reynolds, R., Blichert-Toft, J., Kurz, M.D., 2002. Volcanic evolution in the Galapagos: the dissected shield of Volcano Ecuador. Geochem. Geophys. Geosyst. 3 (10), 1061. doi:10.1029/2002GC000355.

Hildenbrand, A., Marlin, C., Conroy, A., Gillot, P.-Y., Filly, A., Massault, M., 2005. Isotopic approach of rainfall and groundwater circulation in the volcanic structure of Tahiti-Nui (French Polynesia). J. Hydrol. 302, 187–208.

Hürlimann, M., Ledesma, A., Marti, J., 1999. Conditions favouring catastrophic landslides on Tenerife (Canary Islands). Terra Nova 11, 106–111.

Huttel, C., 1995. Vegetación en Coladas de Lava, Islas Galápagos, Ecuador. Fundación Charles Darwin (Eds), Quito.

INGALA, ORSTOM, PRONAREG, 1987. Inventario Cartográfico de los Recursos Naturales, Geomorfología, Vegetación, Hidricos, Ecológicos y Biofisicos de las Islas Galápagos Ecuador. Ingala Edition, Quito.

Join, J.-L., Folio, J.-L., Robineau, B., 2005. Aquifers and groundwater within active shield volcanoes. Evolution of conceptual models in the Piton de la Fournaise volcano. J. Volcanol. Geotherm. Res. 147, 187–201.

Jorgensen, F., Sandersen, P.B.E., Auken, E., 2003. Imaging buried Quaternary valleys using the transient electromagnetic method. J. Appl. Geophys. 53, 199–213.

Krivochieva, S., Chouteau, M., 2003. Integrating TDEM and MT methods for characterization and delineation of the Santa Catarina aquifer (Chalco Sub-Basin, Mexico). J. Appl. Geophys. 52, 23–43.

Lénat, J.F., Fitterman, D., Jackson, D.B., Labazuy, P., 2000. Geoelectrical structure of the central zone of Piton de la Fournaise volcano (Réunion). Bull. Volcanol. 62, 75–89.

Lienert, B.R., 1991. An electromagnetic study of Maui's last active volcano. Geophysics. 56, 972–982.

Malheiro, A., 2006. Geological hazards in the Azores archipelago: Volcanic terrain instability and human vulnerability. J. Volcanol. Geotherm. Res. 156, 158–171.

Nascimento Prada, S., Olivera da Silva, M., Cruz, V.J., 2006. Groundwater behaviour in Madeira, volcanic island (Portugal). Hydrogeol. J. 13, 800–812.

Naumann, T., Geist, D., 2000. Physical volcanology and structural development of Cerro Azul volcano, Isabela island, Galapagos: implications for the development of Galapagos-type shield volcanoes. Bull. Volcanol. 61, 497–514.

Palacky, P.J., 1988. Resistivity characteristics of geological targets. In: Nabighian, M.N. (Ed.), Electromagnetic methods in applied geophysics. Society of Exploration Geophysicists, Tulsa.

Peterson, F.L., 1972. Water development on tropic volcanic island. Type example: Hawaii. Groundwater 10, 18–23.

Snell, H., Rea, S., 1999. The 1997-1998 El Niño in Galapagos: can 34 years of data estimate 120 years of pattern? Noticias de Galápagos 60, 11–20.

Sørensen, K.I., Auken, E., 2004. SkyTEM - A new high-resolution helicopter transient electromagnetic system. Explor. Geophys. 35, 191–199.

Stieljes, L., 1988. Hydrogéologie de l'île volcanique océanique de Mayotte (archipel des Comores, océan indien occidental). Hydrogeol. 2, 135–152.

Vacher, H.L., 1988. Dupuit-Ghyben-Herzberg analysis of strip-island lenses. Geol. Soc. Amer. Bull. 100, 580–591.

Viezzoli, A., Christiansen, A.V., Auken, E., Soerensen, K.I., in press. Quasi-3D modeling of airborne TEM data by Spatially Constrained Inversion, Geophysics.

Violette, S., Ledoux, E., Goblet, P., Carbonnel, J.-P., 1995. Hydrologic and thermal modelling of an active volcano: the Piton de la Fournaise, La Réunion Island. J. Hydrol. 191, 37–63.

White, W.M., McBirney, A.R., Duncan, R.A., 1993. Petrology and geochemistry of the Galapagos: portrait of a pathological mantle plume. J. Geophys. Res. 93, 19533–19563.